PUBLISHED VERSION

http://link.aps.org/doi/10.1103/PhysRevD.60.034014

http://hdl.handle.net/2440/12744

Nucleon magnetic moments beyond the perturbative chiral regime

Derek B. Leinweber, Ding H. Lu, and Anthony W. Thomas

Department of Physics and Mathematical Physics and Special Research Centre for the Subatomic Structure of Matter,
University of Adelaide, Australia 5005

The quark mass dependence of nucleon magnetic moments is explored over a wide range. Quark masses currently accessible to lattice QCD, which lie beyond the regime of chiral perturbation theory (χPT), are accessed via the cloudy bag model (CBM). The latter reproduces the leading nonanalytic behavior of χPT, while modeling the internal structure of the hadron under investigation. We find that the predictions of the CBM are succinctly described by the simple formula $\mu_N(m_\pi) = \mu_N^{(0)}/(1 + \alpha m_\pi + \beta m_\pi^2)$, which reproduces the lattice data, as well as the leading nonanalytic behavior of χPT. As this form also incorporates the anticipated Dirac moment behavior in the limit $m_\pi \to \infty$, it constitutes a powerful method for extrapolating lattice results to the physical mass regime. [S0556-2821(99)02415-7]

PACS number(s): 12.39.Ba, 11.30.Rd, 12.38.Gc, 13.40.Em

I. INTRODUCTION

The fundamental theory of the strong interactions, quantum chromodynamics (QCD), is a nonperturbative field theory in which the self-coupling of the gauge field leads to a nontrivial vacuum structure. The complexity of the QCD vacuum is manifest in nonvanishing vacuum expectation values of quark and gluon operator products having vacuum quantum numbers. The only known way to directly calculate the properties of QCD is through the formulation of a lattice gauge theory where the fields are described on a discrete space-time lattice.

The lattice formulation of QCD is well established [1]. Recent advances in lattice action improvement on anisotropic lattices are greatly facilitating the reduction of systematic uncertainties associated with the finite lattice volume and the finite lattice spacing. However, direct simulation of QCD for light current quark masses, near the chiral limit, remains computationally intensive. As such, the present approach of calculating the properties of QCD using quark masses away from the chiral regime and extrapolating to the physical world is likely to persist for the foreseeable future.

The difficulty associated with this approach is illustrated by the rapid rise of the pseudoscalar mass for small increases in the quark mass away from the chiral limit as governed by

$$m_\pi^2 = -2m_q \frac{\langle 0|\bar{q}q|0 \rangle}{f_\pi^2}, \qquad (1)$$

where q denotes a light quark. Typical quark masses considered in lattice simulations place $m_\pi \sim 500$ MeV, a value significantly larger than the physical pion mass, $\mu = 139.6$ MeV. A mass the order of 500 MeV is sufficient to largely suppress the pion cloud contribution to hadronic observables, whereas near the chiral limit, the pion cloud can make a significant contribution to them [2]. Hence it is imperative to extrapolate any observable simulated on the lattice to the physical world using a function motivated by the physics of the pion cloud. Since the pion cloud contributions are small in lattice simulations, one has to look beyond the lattice simulation results at present.

Historically, lattice results were often linearly extrapolated with respect to m_π^2 to the chiral limit, particularly in exploratory calculations. More recently the focus has turned to chiral perturbation theory (χPT), which provides predictions for the leading nonanalytic quark-mass dependence of observables in terms of phenomenological parameters [3–11].

Application of χPT to the extrapolation of lattice simulation data is now standard for hadron masses and decay constants [1]. However, earlier attempts [12] to apply χPT predictions for the quark-mass dependence of baryon magnetic moments failed, as the higher order terms of the chiral expansion quickly dominate the truncated expansion as one moves away from the chiral limit. To one meson loop, χPT expresses the nucleon magnetic moments as [13,14]

$$\mu_N = \mu_0 + c_1 m_\pi + c_2 m_\pi^2 \log m_\pi^2 + c_3 m_\pi^2 + \cdots, \qquad (2)$$

where μ_0 and c_3 are fitted phenomenologically and c_1 and c_2 are predicted by χPT. The $m_\pi^2 \log m_\pi^2$ term quickly dominates as m_π moves away from the chiral limit, making contact with the lattice results untenable.

Lattice QCD results for baryon magnetic moments [15–17] remain predominantly based on linear quark mass (or m_π^2) extrapolations of the moments expressed in natural magnetons. This approach systematically underestimates the measured moments by 10%–20%. Finite lattice volume and spacing errors are expected to be some source of systematic error. However, χPT clearly indicates that the linear extrapolation of the simulation results is also suspect. As such, it is imperative to find a method which can bridge the void between the realm of χPT and lattice simulations.

We report such a method, which provides predictions for the quark mass (or m_π^2) dependence of nucleon magnetic moments well beyond the chiral limit. In particular, we use the cloudy bag model (CBM), which involves a relativistic quark model (the MIT bag) coupled to the pion field in such a way as to restore chiral symmetry [18,19]. The corresponding pion loop corrections to physical observables reproduce

the leading non-analytic behavior of χPT. However, the loop which gives rise to the leading non-analytic behavior involves two pion propagators. Because the loop is regulated by a form factor, related to the finite size of the hadron, its contribution is suppressed like $1/m_\pi^4$ as m_π becomes large. This feature makes it possible to address the larger quark masses simulated in lattice QCD in a convergent way.

With some tuning of the bag radius, the form factor at the πNN vertex and the current quark mass, within the framework of the CBM, we find that it is possible to reproduce the lattice QCD simulations of nucleon magnetic moments and smoothly extrapolate to the experimentally measured values. We then propose a simple phenomenological relation designed to reproduce the leading nonanalytic structure of χPT and provide the Dirac-moment mass dependence in the heavy quark-mass regime. Finally, we illustrate how such a relation can be used in future lattice QCD calculations. These results may also be useful in clarifying issues surrounding the higher order terms of the chiral expansion of χPT.

II. LATTICE QCD SIMULATION DATA

We consider two independent lattice simulations of the nucleon electromagnetic form factors. Both calculations employ three-point function based techniques [20] utilizing the conserved vector current such that no renormalization is required in relating the lattice results to the continuum. Reference [15] utilizes 28 quenched gauge configurations on a $24\times12\times12\times24$ periodic lattice at $\beta=5.9$, corresponding to a lattice spacing of 0.128(10) fm. Moments are obtained from the form factors at 0.16 GeV^2 by assuming equivalent q^2 dependences for the electric and magnetic form factors. Reference [16] utilizes 12 quenched gauge configurations on a $16^3\times24$ periodic lattice at $\beta=6.0$. The nucleon mass [21] corresponds to a lattice spacing of 0.091(3) fm. Moments are obtained from dipole fits to the form factors. Uncertainties are statistical in origin and are estimated by a single elimination jackknife [22]. Despite having different lattice volumes and lattice spacings, the results from the two calculations agree well within errors. However, experience suggests that the lattice spacings and volumes used in these investigations may give rise to scaling violations and finite size effects the order of 15%–20% from the infinite volume continuum limit.

Ideally, one would like to perform the analysis of chiral corrections, using results from full QCD, as opposed to quenched QCD. Unfortunately, such results are not yet available. Instead we will utilize these results under the standard approach of correcting the lattice scale by fixing the lattice spacing using the nucleon mass. In the absence of any known way to correct for the nonperturbative effects of quenching, we will assume that these lattice results are a reasonable representation of full QCD. Since the quark masses simulated on the lattice are somewhat heavy, the dominant contributions from quark loops neglected in the quenched approximation are largely perturbative and accounted for in the renormalization of the lattice spacing. As we shall see, the errors due to quenching are likely the same order of magni-
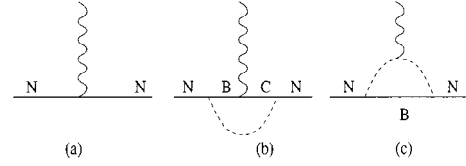

FIG. 1. Schematic illustration of the processes included in the CBM calculation. B and C denote intermediate state baryons and include N and Δ.

tude as the statistical uncertainties.

III. CLOUDY BAG MODEL

The linearized CBM Lagrangian with pseudoscalar pion-quark coupling (to order $1/f_\pi$) is given by [18,19]

$$\mathcal{L}=[\bar{q}(i\gamma^\mu\partial_\mu-m_q)q-B]\theta_V-\frac{1}{2}\bar{q}q\,\delta_S$$

$$+\frac{1}{2}(\partial_\mu\boldsymbol{\pi})^2-\frac{1}{2}m_\pi^2\boldsymbol{\pi}^2-\frac{i}{2f_\pi}\bar{q}\gamma_5\boldsymbol{\tau}\cdot\boldsymbol{\pi}q\,\delta_S, \qquad (3)$$

where B is the bag constant, f_π is the π decay constant, θ_V is a step function (unity inside the bag volume and vanishing outside) and δ_S is a surface delta function. In a lowest order perturbative treatment of the pion field, the quark wave function is not affected by the pion field and is simply given by the MIT bag solution [23]. Our calculation is carried out in the Breit frame with the center-of-mass correction for the bag performed via Peierls-Thouless projection. The detailed formulas for calculating nucleon electromagnetic form factors in the CBM are given in Ref. [24].

In the CBM, a baryon is viewed as a superposition of a bare quark core and bag plus meson states. Both the quark core and the meson cloud contribute to the baryon magnetic moments. These two sources are balanced around a bag radius, $R=0.7$–1.1 fm [25]. A large bag radius suppresses the contributions from the pion cloud, and enhances the contribution from the quark core. The minimal coupling principle is used for the electromagnetic interaction. The nucleon magnetic moments can be written as $\mu_N=G_M^{(q)}(0)+G_M^{(\pi)}(0)$, where $G_M^{(q)}$ is due to γqq coupling and $G_M^{(\pi)}$ from $\gamma\pi\pi$ coupling. To one loop, the CBM reproduces the leading nonanalytic behavior of χPT. The processes included in this calculation are illustrated in Fig. 1.

For the πNN vertex, we take the conventional πNN coupling constant, $f_{\pi NN}^2=0.0771$. Instead of the generic form, the πNN form factor is replaced by the phenomenological, monopole form, $u(k)=(\Lambda^2-\mu^2)/(\Lambda^2+k^2)$, where k is the loop momentum and Λ is a cut-off parameter.

In the standard CBM treatment, where the pion is treated as an elementary field, the current quark mass, m_q, is not directly linked to m_π. Most observables are not sensitive to this parameter, as long as it is in the range of typical current quark masses. For our present purpose it is vital to relate the m_q inside the bag with m_π. Current lattice simulations indicate that m_π^2 is approximately proportional to m_q over a wide range of quark masses [26]. Hence, in order to model the
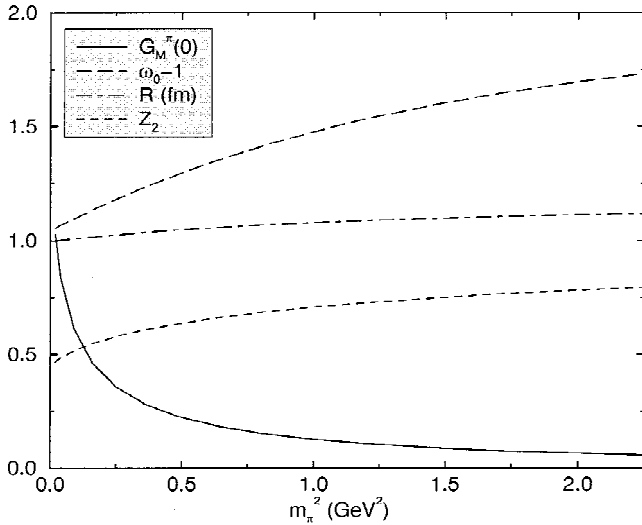
FIG. 2. The pion contribution to the proton magnetic moment $G_M^\pi(0)$ and the properties of the bag including the bare bag probability Z_2, the ground state frequency ω_0, and the bag radius R in variation with the pion mass.

lattice results, we scale the mass of the quark confined in the bag as $m_q = (m_\pi/\mu)^2 m_q^{(0)}$, with $m_q^{(0)}$ being the current quark mass corresponding to the physical pion mass. $m_q^{(0)}$ is treated as an input parameter to be tuned and lies in the range 6 to 7 MeV.

The parameters of the CBM are obtained as follows. The bag constant B and the phenomenological parameter z_0 are fixed by the physical nucleon mass and the stability condition, $dM_N/dR = 0$, for a given R_0 and $m_q^{(0)}$. For each subsequent value of the pion mass or the quark mass considered, ω_0 and R are determined simultaneously from the linear boundary solution of the bag [23] and the stability condition, which provides $R^4 = (3\omega_0 - z_0)/(4\pi B)$. Using the lattice data and the experimental measurement, the parameters R_0, Λ and $m_q^{(0)}$ are tuned to reproduce the experimental moment while accommodating the lattice data.

Figure 2 shows the mass dependence of the bag model properties and the pion-cloud contribution $G_M^\pi(0)$. The bare bag probability, Z_2, the quark ground state frequency, ω_0, and the bag radius, R, are plotted as a function of m_π^2. As m_π increases, the pion-cloud contribution decreases very quickly and becomes quite small for large quark masses—especially in the range corresponding to the current lattice calculations. On the other hand, the bag properties evolve relatively slowly. As a result, the dominant influences of R_0, Λ governing the πNN coupling, and $m_q^{(0)}$ are located in separate regions of m_π. The magnitude of the magnetic moments in the small m_π region is controlled by Λ and R_0, while a variation of $m_q^{(0)}$ is more effective in the large m_π region, where the pion cloud nearly vanishes.

IV. DISCUSSION OF RESULTS

The nucleon magnetic moments calculated in the CBM are shown in Fig. 3 for the proton and Fig. 4 for the neutron by the solid line. The lattice results (● [15], ■ [16]) are also
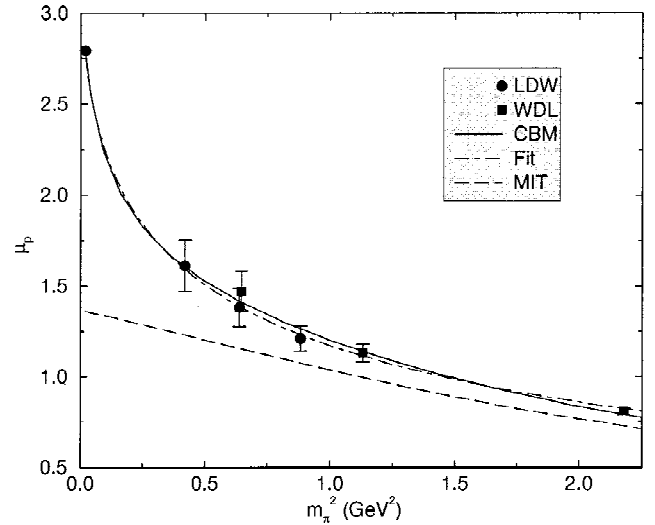

FIG. 3. The proton magnetic moment as calculated in lattice QCD (● LDW [15], ■ WDL [16]), the cloudy bag model (CBM) which includes the pion cloud contribution and the MIT bag model (MIT) where the pion cloud contribution of the CBM is omitted. Also illustrated is a fit of the simple analytic form of Eq. (4) to the CBM results. The point at the physical value of m_π^2 is the experimental measurement and is used to constrain the parameters of the CBM.

plotted in these figures. It is possible to simultaneously reproduce the existing lattice simulation results for the nucleon magnetic moments at large m_π as well as their physical values using CBM parameters within previously established ranges. These parameters are summarized in Table I. The dashed lines in Figs. 3 and 4 indicate the corresponding results for the MIT bag model. There, without the pion cloud, the m_π^2 dependence of the magnetic moments becomes nearly linear. This clearly shows the significance of the meson cloud, especially in the small m_π regime.

Since the pion cloud in the quenched approximation is quite different from that of full QCD [3–6,27], one might
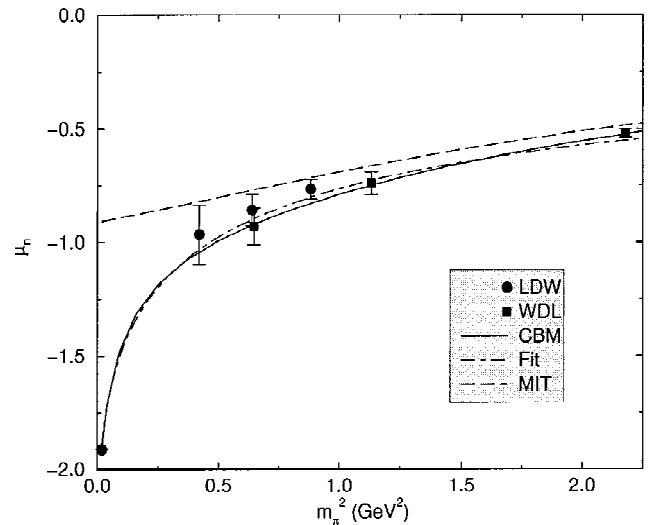

FIG. 4. The neutron magnetic moment. Symbols and lines are as described for Fig. 3.

TABLE I. CBM parameters and optimal fit parameters for the fit function of Eq. (4). Other CBM parameters are $Z_0 = 2.59$ and $B^{1/4} = 144$ MeV. At physical pion mass, the experimental magnetic moments (2.79 and -1.91 for the proton and neutron) are reproduced in the CBM.

N	R_0 (fm)	Λ (GeV)	$m_q^{(0)}$ (MeV)	$\mu_N^{(0)}$	α (GeV^{-1})	β (GeV^{-2})
Proton	1.0	0.68	4.8	3.31	1.37	0.452
Neutron	1.0	0.59	4.8	-2.39	1.85	0.271

regard the difference between the CBM and MIT model results (i.e. the pion contribution) as indicative of the absolute systematic error associated with the quenched approximation. For the quark masses actually simulated on the lattice, this error is the order of 15%. However, some of this difference is already accounted for in the lattice results through a renormalization of the lattice spacing used in expressing the moments in nuclear magnetons. Hence, for the purposes of this investigation, it is reasonable to accept the quenched results as an approximate representation of the full QCD result.

V. ENCAPSULATING FORM

Having established the quark mass dependence of the nucleon moments over a very wide range, we now turn to encapsulating these results in a simple analytic form that might be used in future lattice QCD extrapolations of simulation results. The function

$$\mu_N(m_\pi) = \frac{\mu_N^{(0)}}{1 + \alpha m_\pi + \beta m_\pi^2} \qquad (4)$$

is matched to the CBM model results by tuning the three parameters $\mu_N^{(0)}$, α and β. These fits are also illustrated in Figs. 3 and 4. This functional form provides the correct limiting behavior as a function of m_π. As $m_\pi \to 0$, Eq. (4) may be expanded as

$$\mu_N(m_\pi) = \mu_N^{(0)}[1 - \alpha m_\pi + (\alpha^2 - \beta)m_\pi^2 + \cdots], \qquad (5)$$

such that the leading nonanalytic behavior is proportional to m_π as required by χPT. For large m_π, Eq. (4) leads to

$$\mu_N(m_\pi) = \frac{\mu_N^{(0)}}{\beta m_\pi^2}\left(1 - \frac{\alpha}{\beta m_\pi} + \cdots\right), \qquad (6)$$

such that the magnetic moments decrease as $1/m_q$ for increasing quark mass, precisely as the Dirac moment requires. In short, this function reproduces the leading nonanalytic behavior of χPT, provides the desired mass dependence of the Dirac moment in the heavy quark mass limit and also has the required shape in our region of interest. The resulting parameters for this fit are also listed in Table I.

Because the leading nonanalytic terms predicted in χPT for baryon magnetic moments are proportional to the pseudoscalar meson mass, the kaon cloud is often regarded as the most important and dominant contribution. Instead, in the CBM with its natural high momentum cutoff, the overall contribution of the kaon loop is strongly suppressed. More-

over, the kaon cloud contribution to the nucleon magnetic moments will not display the same significant curvature associated with the pion cloud. In consequence, the kaon cloud contributions may simply be absorbed into the fit parameters $\mu_N^{(0)}$ and β.

To evaluate the ability of Eq. (4) to encompass the CBM predictions, the lattice QCD data and maintain the correct leading nonanalytic behavior of χPT, we compare the coefficient of m_π in Eq. (5) with that predicted by χPT. Table II summarizes numerical values for this coefficient. The one-loop corrected estimates for the D and F coefficients provide better agreement between χPT and experiment for many observables [13]. The similarity between this χPT estimate and the coefficient from the encapsulating form is encouraging.

VI. EXTRAPOLATION OF LATTICE QCD DATA

Future lattice QCD studies of octet baryon magnetic moments will make better contact with experiment by adopting the one-loop corrected coefficient of m_π from χPT and performing a two parameter fit of Eq. (4) to the simulation data [28]. The utility of this approach is illustrated in Fig. 5. The nucleon magnetic moments at the physical pion mass obtained from this extrapolation are

$$\mu_p = 2.85(22)\mu_N \quad \text{and} \quad \mu_n = -1.90(15)\mu_N \qquad (7)$$

and agree surprisingly well with the experimental measurements, 2.793 and $-1.913\ \mu_N$ respectively. The fit parameters $(\mu^{(0)}, \beta)$ in units of (μ_N, GeV^{-2}) are $(3.39(23), 0.58(16))$ and $(-2.40(16), 0.41(16))$ for the proton and neutron respectively. We note that the data required

TABLE II. Values for the coefficient of the leading nonanalytic term obtained from the chiral expansion of Eq. (4) adjusted to fit the CBM results for the proton and neutron and from χPT. $\mu_N^{(0)}$ and α are from Table I. D_0 and F_0 are tree-level coefficients ($D_0 + F_0 = g_A = 1.27$) while D_1 and F_1 are the one-loop corrected estimates of Ref. [13]. Units are GeV^{-1}. In the column headings, the upper and lower signs correspond to the proton and neutron respectively.

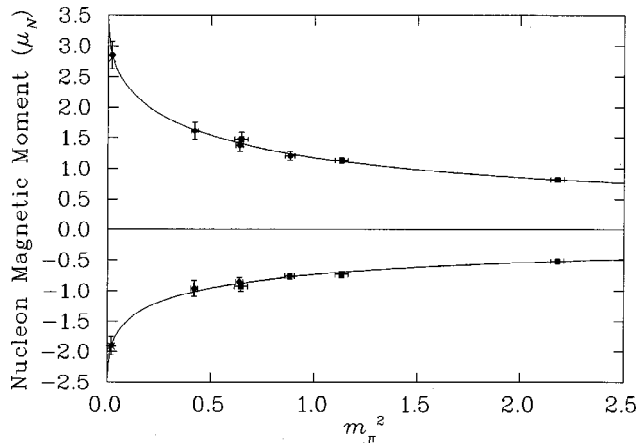| Nucleon		Chiral perturbation theory	
	Encapsulating form $-\mu_N^{(0)}\alpha$	$\mp\dfrac{m_N(D_0+F_0)^2}{8\pi f_\pi^2}$	$\mp\dfrac{m_N(D_1+F_1)^2}{8\pi f_\pi^2}$
Proton	-4.54	-6.97	-4.41
Neutron	4.42	6.97	4.41

FIG. 5. Extrapolation of lattice QCD magnetic moments (● LDW [15], ■ WDL [16]) for the proton (upper) and neutron (lower) to the chiral limit. The curves illustrate a two parameter fit of Eq. (4) to the simulation data in which the one-loop corrected chiral coefficient of m_π is taken from χPT. The experimentally measured moments are indicated by asterisks.

to do a fit of the lattice results in which covariances are taken into account are no longer available. As such, the uncertainties quoted here should be regarded as indicative only.

VII. CONCLUSIONS

In summary, we have explored the quark mass dependence of nucleon magnetic moments. Quark masses beyond the regime of chiral perturbation theory have been accessed via the cloudy bag model which reproduces the leading nonanalytic behavior of χPT and provides internal structure for the hadron under investigation. We find that the predictions of the CBM are succinctly described by a simple formula which reproduces the leading nonanalytic behavior of χPT in the limit $m_\pi \to 0$ and provides the anticipated Dirac moment behavior in the limit $m_\pi \to \infty$. The significance of nonlinear behavior in extrapolating nucleon magnetic moments as a function of m_q to the chiral regime has been evaluated. We find that the leading nonanalytic term of the chiral expansion dominates from the chiral limit up to the physical pion mass. Beyond the physical mass, higher order terms become important and dominate. This curvature, neglected in previous linear extrapolations of the lattice data, can easily account for the departures of earlier lattice estimates from experimental measurements. As finite volume and lattice spacing artifacts are eliminated in future lattice QCD simulations, it will be interesting to see if the fit parameters adjust accordingly to maintain and perhaps improve the level of agreement seen in this investigation. We advocate the use of the function in Eq. (4) in future lattice QCD investigations of octet baryon magnetic moments.

[1] *Lattice '98*, Proceedings of the International Symposium, Boulder, Colorado, 1998, edited by T. DeGrand, C. DeTar, R. Sugar, and D. Toussaint, [Nucl. Phys. B (Proc. Suppl.), (in press)].

[2] D. B. Leinweber and T. D. Cohen, Phys. Rev. D **47**, 2147 (1993); A. W. Thomas, Aust. J. Phys. **44**, 173 (1991).

[3] M. F. L. Golterman, Acta Phys. Pol. B **25**, 1731 (1994).

[4] J. N. Labrenz and S. R. Sharpe, Nucl. Phys. B (Proc. Suppl.) **34**, 335 (1994).

[5] C. Bernard and M. Golterman, Phys. Rev. D **46**, 853 (1992).

[6] S. R. Sharpe, Phys. Rev. D **46**, 3146 (1992).

[7] B. Holstein, in *Future Directions in Quark Nuclear Physics*, CSSM, Adelaide, SA, 1998, edited by K. Tsushima and A. W. Thomas (World Scientific, Singapore, 1998), nucl-th/9806037.

[8] P. Langacker and H. Pagels, Phys. Rev. D **8**, 4595 (1973).

[9] S. Weinberg, Physica A **96**, 327 (1979).

[10] J. Gasser and H. Leutwyler, Ann. Phys. (N.Y.) **158**, 142 (1984).

[11] J. Gasser, M. E. Sainio, and A. Suarc, Nucl. Phys. **B307**, 779 (1988).

[12] M. Butler, D. B. Leinweber, and R. Springer (unpublished).

[13] E. Jenkins, M. Luke, A. V. Manohar, and M. J. Savage, Phys. Lett. B **302**, 482 (1993); **388**, 866(E) (1996).

[14] L. Durand and P. Ha, Phys. Rev. D **58**, 013010 (1998).

[15] D. B. Leinweber, R. M. Woloshyn, and T. Draper, Phys. Rev. D **43**, 1659 (1991).

[16] W. Wilcox, T. Draper, and K. F. Liu, Phys. Rev. D **46**, 1109 (1992).

[17] S. J. Dong, K. F. Liu, and A. G. Williams, Phys. Rev. D **58**, 074504 (1998).

[18] S. Théberge, A. W. Thomas, and G. A. Miller, Phys. Rev. D **22**, 2838 (1980); **23**, 2106(E) (1981).

[19] A. W. Thomas, in *Advances in Nuclear Physics*, edited by J. Negle and E. Vogt (Plenum, New York, 1984), Vol. 13, p. 1; G. A. Miller, Int. Rev. Nucl. Phys. **2**, 90 (1984).

[20] Magnetic moment contributions from the coupling of the electromagnetic current directly to sea-quark loops are neglected in these simulations. However, the net effect from u, d, and s sea-quark loops is small due to approximate SU(3)-flavor symmetry where the net loop contribution vanishes.

[21] S. Cabasino *et al.*, Nucl. Phys. B (Proc. Suppl.) **20**, 399 (1991).

[22] B. Efron, SIAM (Soc. Ind. Appl. Math.) Rev. **21**, 460 (1979).

[23] A. Chodos *et al.*, Phys. Rev. D **9**, 3471 (1974); A. Chodos *et al.*, *ibid.* **10**, 2599 (1974); T. A. DeGrand *et al.*, *ibid.* **12**, 2060 (1975).

[24] D. H. Lu, A. W. Thomas, and A. G. Williams, Phys. Rev. C **57**, 2628 (1998).

[25] S. Théberge and A. W. Thomas, Nucl. Phys. **A393**, 252 (1983).

[26] S. Aoki *et al.*, in *Lattice '97,* Proceedings of XVth International Symposium on Lattice Field Theory, Edinburgh, UK, 1997, edited by C. T. H. Davies *et al.* [Nucl. Phys. B (Proc. Suppl.) **60A**, 14 (1998)].

[27] T. D. Cohen and D. B. Leinweber, Comments Nucl. Part. Phys. **21**, 137 (1993).

[28] This dependence on χPT will eventually be alleviated as better lattice data become available at smaller quark masses, allowing a three parameter fit of Eq. (4).